Proceedings of the Twenty-fourth (2014) International Ocean and Polar Engineering Conference **www.isope.org**
Busan, Korea, June 15-20, 2014

ISBN 978-1 880653 91-3 (Set); ISSN 1098-6189 (Set)

Modeling the Stress-Strain Properties of Synthetic Fiber Mooring Lines under Cyclic Loading

Wei Huang
Deepwater Technology Research Centre (DTRC), Bureau Veritas Marine (Singapore) Pte Ltd.
Singapore
Haixiao Liu
Civil Engineering, Tianjin University.
Tianjin, China
Cun Hu
Institute of Mechanics, Chinese Academy of Sciences.
Beijing, China

ABSTRACT

The nonlinear stress-strain relationship of synthetic fiber ropes under cyclic loading is a property of vital importance which directly influences the dynamic tension response of mooring lines. How to capture the load-elongation relationship of the synthetic fiber mooring lines under cyclic loading and obtain the quantitative description is a key problem which would be of interest to mooring system designers, platform operators and researchers. The former studies were insufficient to take into account the true loading history, creep behavior and the evolution of the dynamic stiffness. A viscoelastic and viscoplastic model is developed herein to describe the stress-strain properties of synthetic fiber mooring lines. The total strain is decomposed into a recoverable viscoelastic strain and an irrecoverable plastic strain. The time-dependent property and the evolution of the dynamic stiffness can be fully incorporated in the developed model. The model is examined by comparing with the experimental results of polyester ropes under both creep-recovery and sinusoidal loadings. Through a detailed parametric analysis, further knowledge of the hysteresis loop and the dynamic stiffness evolution is clearly obtained. The present work is beneficial to improving the understanding of the performance of synthetic fiber ropes, and also provides a better basis for the further research on the mechanical problems of synthetic fiber mooring lines under complicated loading conditions.

KEY WORDS: Synthetic fiber mooring line; stress-strain property; dynamic stiffness; time-dependent behavior; evolution; loading history; cyclic loading.

INTRODUCTION

A mooring system will be designed so that it has sufficient stiffness to keep the floating offshore platforms from drifting too far off station while having enough compliance to avoid overload in the mooring lines, which is resulted from the motions of the platform under the influence of the external forces caused by the complicated sea environment. Since the first installation of floating production systems by Petrobras in 1997, synthetic fiber ropes are extensively used as mooring lines for the station-keeping of floating platforms in deep waters. The taut-wire mooring system (TMS) using synthetic fiber ropes has become a very attractive alternative to the conventional steel catenary system (Nielsen and Bindingbø, 2000). However, due to the mechanical properties of synthetic fiber ropes, the performance and response of this type of mooring system subjected to cyclic loading become more complicated. Evaluating the response of the TMS, the adequacy of the maximum offset and the line tensions with the relevant acceptable criteria, requires a description of the load-elongation properties, i.e., the stress-strain properties of synthetic fiber ropes. However, these properties are rather complex to evaluate and specify, in comparison with the linear elastic behavior of the equivalent steel components, because they are both nonlinear and time-dependent (François *et al.*, 2010). The stress-strain relationship of the synthetic fiber ropes under cyclic loading shows significant nonlinear behavior such as hysteresis because of viscoelasticity and viscoplasticity of the material. Based on an experimental investigation, it was observed that the hysteresis loops of the stress-strain curve superimposed each other and became stable after the mooring line experienced a certain number of cycles. This is the dynamic stiffness of synthetic fiber ropes which shows significant difference from the material properties of steel chains or wire ropes. Besides, the synthetic fiber ropes also will exhibit creep and relaxation behavior, which increase the complexity of the evolution of dynamic stiffness that directly relates to the tension response.

Therefore, during almost 20 years for the development of the TMS, a number of experimental and numerical studies were performed to figure out the dynamic stiffness through different ways. An empirical equation was proposed by Del Vecchio (1992) based on model experiments for determining the stable rope modulus after sufficient cycles at a constant temperature, as a function of several influential parameters. With this formula serving as a starting point, other researchers performed more model experiments to improve it and tried

to investigate the parametric effects. Bosman and Hooker (1999) investigated the dynamic stiffness of 3-strand polyester sub-ropes with breaking strength of 11.25t and full-size polyester ropes with breaking strength of 150t. It was observed that the mean load was the main factor that influences the dynamic modulus. Similar experimental studies on ropes with different sizes or loading conditions also can be found in the literature (Casey et al., 2000; François and Davies, 2000; Casey and Banfield, 2002; Davies et al., 2002; Casey and Banfield, 2005; Wibner et al., 2003; Davies et al., 2008; François and Davies, 2008). The main objective of these studies was restricted to obtaining a stable modified dynamic stiffness for the fiber ropes under cyclic loading. Thus, on the one hand, this approach cannot fully take into account the multifactor effects on the dynamic stiffness; on the other hand, the true loading history and the stiffness evolution cannot be incorporated in the approach. Additionally, Bitting (1985) tried to describe the dynamic stress-strain relationship of the nylon and polyester double braid lines by a three-parameter model involved spring and dashpot elements, but there were difficulties and uncertainties in the estimation of the response coefficients. Flory et al. (2004, 2007) proposed a spring-dashpot model to represent the change-in-length properties of the polyester fiber ropes under several different loading sequences, but it was just used to qualitatively describe the properties and the similar difficulties also existed in determining the coefficients. François and Davies (2008) studied the characterization of polyester mooring lines and pointed out that the development of a true "time domain" rheological model and a definitive understanding of underlying mechanism required further efforts; creep behavior was an important property due to the viscoelasticity and viscoplasticity of fiber ropes and would influence the evolution of the dynamic stiffness. Chailleux and Davies (2003, 2005) proposed a model to describe the creep behavior of aramid and polyester fibers. Actually, the viscoelastic and viscoplastic property also exists in many other materials such as the HDPE (High-Density Polyethylene) (Lai and Bakker, 1995; Lai and Bakker, 1996; Haj-Ali and Muliana, 2004; Kim and Muliana, 2009), the epoxy polymer (Xia et al., 2005), and the asphalt sand (Ye et al., 2010). The constitutive models for these materials make significant reference to the present work.

STRESS-STRAIN CONSTITUTIVE MODEL

Because the synthetic fiber mooring lines show obvious viscoelasticity and viscoplasticity, the Schapery thermodynamic theory and a viscoplastic function are employed. We assume that the total strain $\varepsilon(t)$ is the sum of a recoverable viscoelastic strain $\varepsilon_{ve}(t)$ and an irrecoverable plastic strain $\varepsilon_{vp}(t)$, which can be represented as:

$$\varepsilon(t) = \varepsilon_{ve}(t) + \varepsilon_{vp}(t) \tag{1}$$

The current recoverable strain is dependent on the whole loading history and can be represented by the single integral constitutive equation developed by Schapery, which is a macroscopic model based on thermodynamic assumptions. The Schapery theory is capable of describing the strong nonlinearity where the time-dependence and stress-dependence of the creep compliance are not separable. For uniaxial deformation under isothermal condition, the Schapery integral form (Lai and Bakker, 1995; Lai and Bakker, 1996) for the current viscoelastic strain can be expressed by:

$$\varepsilon_{ve} = g_0 D_0 \sigma(t) + g_1 \int_0^t \Delta D[\psi(t) - \psi(\tau)] \frac{d(g_2\sigma)}{d\tau} d\tau \tag{2}$$

where, $\sigma(t)$ denotes the stress at time t; g_0 denotes the nonlinear instantaneous elastic compliance which measures the increase and reduction in stiffness; g_1 denotes the transient creep parameter which measures the nonlinear effect in the transient compliance; g_2 denotes the load rate effect parameter on the creep response; D_0 and $\Delta D(\psi)$ are the instantaneous and transient creep compliances; ψ is the reduced time defined by:

$$\psi(t) = \int_0^t \frac{ds}{a_\sigma[\sigma(s)]} \tag{3}$$

in which a_σ denotes the time scaling parameter; the nonlinear material properties g_0, g_1, g_2, and a_σ are all functions of stress. It should be noted that these functions are always positive and equal one for relatively small values of stress magnitudes. In other words, when all these functions equal one, Eq. (2) corresponds to Boltzmann's superposition principle and the material exhibits linear viscoelastic behavior. The transient compliance ΔD can be expressed using the Prony series (Haj-Ali and Muliana, 2004) as:

$$\Delta D(\psi) = \sum_{n=1}^{N} D_n \left[1 - e^{(-\lambda_n \psi)}\right] \tag{4}$$

where, N is the number of the terms; D_n is the nth coefficient of the Prony series; λ_n is the nth reciprocal of retardation time.

Accounting for the following creep-recovery stress history:

$$\sigma(t) = \begin{cases} \sigma_c & 0 < t \le t_1 \\ 0 & t_1 < t \le t_2 \end{cases} \tag{5}$$

where $\sigma = 0$, if $t < 0$; σ_c is a constant. If $0 < t \le t_1$, Eq. (2) can be reduced to:

$$\varepsilon_{ve}(t) = g_0 D_0 \sigma_c + g_1 g_2 \sigma_c \Delta D[\psi(t)] \tag{6}$$

where $\psi(t) = t / a_\sigma(t)$. If $t_1 < t \le t_2$, Eq. (2) can be reduced to:

$$\varepsilon_{ve}(t) = g_2 \sigma_c \{\Delta D[\psi_1(t)] - \Delta D[\psi_2(t)]\} \tag{7}$$

where $\psi_1(t) = t_1 / a_\sigma + t - t_1$; $\psi_2(t) = t - t_1$.

Substituting Eq. (4) into Eq. (6) yields:

$$\varepsilon_{ve}(t) = g_0 D_0 \sigma_c + g_1 g_2 \sigma_c \sum_{n=1}^{N} D_n \left[1 - e^{(-\lambda_n t / a_\sigma)}\right] \tag{8}$$

Substituting Eq. (4) into Eq. (7) yields:

$$\varepsilon_{ve}(t) = g_2 \sigma_c \left\{ \sum_{n=1}^{N} D_n \left[1 - e^{-\lambda_n (t_1/a_\sigma + t - t_1)}\right] - \sum_{n=1}^{N} D_n \left[1 - e^{-\lambda_n (t - t_1)}\right] \right\} \tag{9}$$

When considering a creep-recovery stress history, the analytical expression of the strain can be obtained directly. However, if we account for a sinusoidal loading history, a numerical iterative procedure is needed to complete the integration of the nonlinear viscoelastic model. Substituting Eq. (4) into Eq. (2) yields:

$$\varepsilon_{ve}(t) = \varepsilon_{ve}^0(t) - g_1(t) \sum_{n=1}^{N} D_n q_n(t) \tag{10}$$

where:

$$\varepsilon_{ve}^0(t) = [g_0(t) D_0 + g_1(t) g_2(t) \sum_{n=1}^{N} D_n] \sigma(t) \tag{11}$$

$$q_n(t) = \int_0^t e^{\{-\lambda_n [\psi(t) - \psi(\tau)]\}} \frac{d[g_2(\tau)\sigma(\tau)]}{d\tau} d\tau \tag{12}$$

By dividing Eq. (12) into two parts considering a time step Δt, a recursive integration form can be obtained. The first part includes the integral with limits (0, $t - \Delta t$), and the limits of the second part are taken as ($t - \Delta t$, t), where t is the current time. Thus:

$$q_n(t) = \int_0^{t-\Delta t} e^{\{-\lambda_n [\psi(t) - \psi(\tau)]\}} \frac{d[g_2(\tau)\sigma(\tau)]}{d\tau} d\tau + \int_{t-\Delta t}^{t} e^{\{-\lambda_n [\psi(t) - \psi(\tau)]\}} \frac{d[g_2(\tau)\sigma(\tau)]}{d\tau} d\tau \tag{13}$$

The reduced time increment $\Delta\psi$ is given by:

$$\Delta\psi(t)=\psi(t)-\psi(t-\Delta t) \tag{14}$$

The first integral on the right side of Eq. (13) can be written as:

$$\int_0^{t-\Delta t} e^{\{-\lambda_n[\psi(t)-\psi(\tau)]\}}\frac{d[g_2(\tau)\sigma(\tau)]}{d\tau}d\tau = e^{(-\lambda_n\Delta\psi)}q_n(t-\Delta t) \tag{15}$$

$q_n(t-\Delta t)$ in Eq. (15) is the hereditary integral for every term in the Prony series at the end of the previous time $t-\Delta t$, which can be taken into account as the history variables that need to be updated and stored at the end of each time increment. The second term of integral in Eq. (13) is carried out while assuming that the term $g_2(\tau)\sigma(\tau)$ is linear over the current time increment Δt; the shift parameter is not directly a function of time. Then the second integral can be evaluated by:

$$\int_{t-\Delta t}^{t} e^{\{-\lambda_n[\psi(t)-\psi(\tau)]\}}\frac{d[g_2(\tau)\sigma(\tau)]}{d\tau}d\tau = \frac{1-e^{[-\lambda_n\Delta\psi(t)]}}{\lambda_n\Delta\psi(t)}[g_2(t)\sigma(t)-g_2(t-\Delta t)\sigma(t-\Delta t)] \tag{16}$$

Substituting Eqs. (15) and (16) into Eq. (13) leads to:

$$q_n(t)=e^{(-\lambda_n\Delta\psi)}q_n(t-\Delta t)+\frac{1-e^{[-\lambda_n\Delta\psi(t)]}}{\lambda_n\Delta\psi(t)}[g_2(t)\sigma(t)-g_2(t-\Delta t)\sigma(t-\Delta t)] \tag{17}$$

Substituting Eq. (17) in Eq. (10), we obtain the current total viscoelastic strain:

$$\varepsilon_{ve}(t)=\Psi(t)\sigma(t)-\Phi(t) \tag{18}$$

where:

$$\Psi(t)=g_0(t)D_0+g_1(t)g_2(t)\sum_{n=1}^{N}D_n-g_1(t)g_2(t)\sum_{n=1}^{N}D_n\frac{1-e^{[-\lambda_n\Delta\psi(t)]}}{\lambda_n\Delta\psi(t)} \tag{19}$$

$$\Phi(t)=g_1(t)\sum_{n=1}^{N}D_n\{e^{(-\lambda_n\Delta\psi)}q_n(t-\Delta t)-g_2(t-\Delta t)[1-e^{(-\lambda_n\Delta\psi)}]\frac{\sigma(t-\Delta t)}{\lambda_n\Delta\psi}\} \tag{20}$$

Substituting Eq. (17) in Eq. (20), allows $\Phi(t)$ to be rewritten as:

$$\Phi(t)=g_1(t)\sum_{n=1}^{N}D_n\{q_n(t)-g_2(t)\sigma(t)\frac{1-e^{[-\lambda_n\Delta\psi(t)]}}{\lambda_n\Delta\psi(t)}\} \tag{21}$$

$\Phi(t-\Delta t)$ can be then written as:

$$\Phi(t-\Delta t)=g_1(t-\Delta t)\sum_{n=1}^{N}D_n\{q_n(t-\Delta t)-g_2(t-\Delta t)\sigma(t-\Delta t)\frac{1-e^{[-\lambda_n\Delta\psi(t-\Delta t)]}}{\lambda_n\Delta\psi(t-\Delta t)}\} \tag{22}$$

The current viscoelastic incremental strain can be obtained by:

$$\Delta\varepsilon_{ve}(t)=\Delta(\Psi\sigma)-\Delta\Phi \tag{23}$$

where:

$$\Delta(\Psi\sigma)=\Psi(t)\sigma(t)-\Psi(t-\Delta t)\sigma(t-\Delta t) \tag{24}$$

$$\Delta\Phi=\Phi(t)-\Phi(t-\Delta t)=Q+P \tag{25}$$

$$Q=\sum_{n=1}^{N}D_n\{g_1(t)e^{[-\lambda_n\Delta\psi(t)]}-g_1(t-\Delta t)\}q_n(t-\Delta t) \tag{26}$$

$$P=g_2(t-\Delta t)\sum_{n=1}^{N}D_n\{g_1(t-\Delta t)\frac{1-e^{[-\lambda_n\Delta\psi(t-\Delta t)]}}{\lambda_n\Delta\psi(t-\Delta t)}-g_1(t)\frac{1-e^{[-\lambda_n\Delta\psi(t)]}}{\lambda_n\Delta\psi(t)}\}\sigma(t-\Delta t) \tag{27}$$

It should be noticed that the synthetic fiber mooring lines also show viscoplasticity; a plastic function is needed to represent this type of material behavior. The generation of the viscoplastic strain depends on the yield stress level, i.e., σ_y and the application duration of the new stress. We consider a multiple loading history, i.e., $\sigma_1(t_1),\sigma_2(t_2),...,\sigma_i(t_i),...,\sigma_n(t_n)$, the viscoplastic strain will be generated and accumulated if $\sigma_i\geq\sigma_y$, and the plastic strain increment $\Delta\varepsilon_{vp}^i$ due to the stress σ_i for a time Δt_i can be given by:

$$\Delta\varepsilon_{vp}^i=\varepsilon_{vp}(\sigma_i,t_i^e+\Delta t_i)-\varepsilon_{vp}(\sigma_i,t_i^e) \tag{28}$$

where t_i^e denotes the effective time when the plastic deformation starts. The summation of $\Delta\varepsilon_{vp}^i$ yields the total plastic strain resulting from the multiple-step stress:

$$\varepsilon_{vp}(t)=\sum_{i=1}^{n}\Delta\varepsilon_{vp}^i \tag{29}$$

It is observed that the plastic strain function can be represented by the following expression (Zapas and Crissman, 1984):

$$\varepsilon_{vp}(t)=\sigma D_p(\sigma)t^{m(\sigma)} \tag{30}$$

where D_p denotes the plastic strain rate, and m denotes the material parameter of the plastic function. Both of them are stress-dependent. The viscoplastic strain under an arbitrary loading history when $\sigma_i\geq\sigma_y$ can be given by:

$$\varepsilon_{vp}(t)=\int_0^t\sigma(\tau)D_p(\sigma)m(\sigma)\tau^{m(\sigma)-1}d\tau \tag{31}$$

IDENTIFICATION OF PARAMETERS

It is well-known that the parameter identification is a necessary and key part for a developed numerical model. In the constitutive model, six stress-dependent parameters and coefficients of the Prony series must be determined. In this section, a new data-reduction method to determine the nonlinear parameters is proposed. In order to determine the parameters, the experimental results of simple creep-recovery experiments at different stress levels are employed.

Based on Eq. (1) and Eq. (6), the creep strain at $t=0$ can be given by:

$$\varepsilon_c(0)=g_0D_0\sigma_c \tag{32}$$

Then, the creep strain at t_1^-, which is the time just before the unloading in the creep-recovery test, can be given as:

$$\varepsilon_c(t_1^-)=g_0D_0\sigma_c+g_1g_2\Delta D(\frac{t_1^-}{a_\sigma})\sigma_c+\varepsilon_{vp} \tag{33}$$

The recovery strain at t_1^+, which is the time just after the unloading in the creep-recovery test, can be given as:

$$\varepsilon_r(t_1^+)=g_2\Delta D(\frac{t_1^+}{a_\sigma})\sigma_c+\varepsilon_{vp} \tag{34}$$

Following Eqs. (32)~(34), g_1 can be obtained by:

$$g_1=\frac{\varepsilon_c(t_1^-)-\varepsilon_c(0)-\varepsilon_{vp}}{\varepsilon_r(t_1^+)-\varepsilon_{vp}} \tag{35}$$

It should be noted that the parameter g_1 can be easily calculated, as the values of $\varepsilon_c(t_1^-)$, $\varepsilon_c(0)$, $\varepsilon_r(t_1^+)$ and ε_{vp} can be directly experimentally measured from the creep-recovery experiments, as shown in Fig. 1.

Considering the viscoelastic recovery strain, we obtain:

$$\varepsilon_{rve}=\varepsilon_r(t)-\varepsilon_{vp}=g_2\sigma_c\sum_{n=1}^{N}D_n\left[e^{-\lambda_n(t-t_1)}-e^{-\lambda_n\left(\frac{t_1}{a_\sigma}+t-t_1\right)}\right] \tag{36}$$

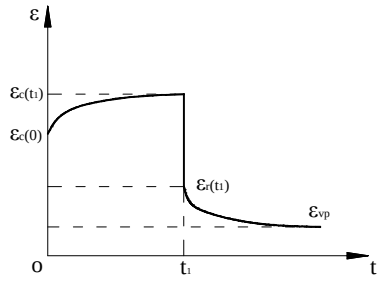

Fig. 1 A typical strain-time curve for a creep and recovery test

If the stress level is sufficiently small, the material exhibits linear

viscoelastic behavior, which means that the parameters g_2 and a_σ all equal one. Combined with the polynomial fitting of the experimental data from the creep-recovery experiments, we can determine the parameters of the Prony series. Repeating the fitting at the higher stress levels, the parameters g_2 and a_σ can be obtained. Note that in order to eliminate the plastic strain from the recovery, the relation proposed by Lai and Bakker (1995) is adopted, i.e., $\varepsilon_{cr} = \varepsilon_c(t_1) - \varepsilon_r(t)$. Therefore, the following expression can be derived as:

$$\varepsilon_{cr}(t) = g_0 D_0 \sigma_c + g_2 \sigma_c \sum_{n=1}^{N} D_n \left[1 - e^{-\lambda_n g_1 \left(\frac{t_1}{a_\sigma} \right)} + e^{-\lambda_n \left(\frac{t_1}{a_\sigma} + t - t_1 \right)} - e^{-\lambda_n (t - t_1)} \right] \quad (37)$$

Fitting Eq. (37) to the experimental data, the parameters g_0 and the material constant D_0 can be determined. After determining all parameters in the viscoelastic model, the viscoplastic strain should be involved to identify the parameters in the plastic function. Thus, the total creep strain can be described by:

$$\varepsilon_c(t) = g_0 D_0 \sigma_c + g_1 g_2 \sigma_c \sum_{n=1}^{N} D_n (1 - e^{-\lambda_n \frac{t}{a_\sigma}}) + D_p \sigma_c t^m \quad (38)$$

By fitting Eq. (38) to the experimental data, the parameters D_p and m can be obtained.

Through the above procedure, all the parameters in the developed model can be determined. Being a demonstration, a single 33t MBL (minimum breaking load) polyester rope with five loading and unloading cycles and corresponding strains is applied to identify the parameters (Davies et al., 2003). For the rope, the loadings were 20%, 30%, 40%, 50%, and 60% MBL; the experimental results are presented in Fig. 2.

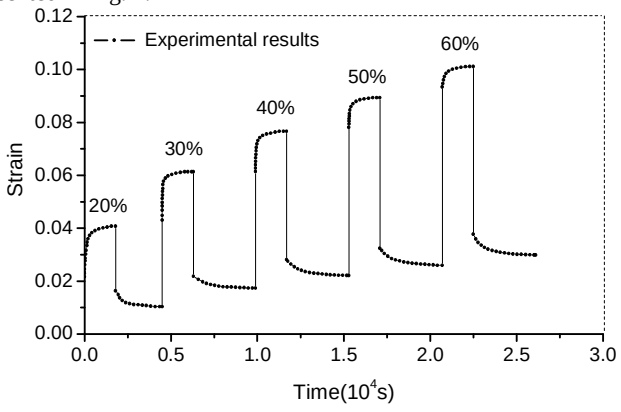

Fig. 2 Experimental results for parameter identification

It was assumed that the material exhibited linear viscoelastic behavior when the stress was below 20% MBL. In this case, the parameters g_0, g_1, g_2, and a_σ all equal 1. In fact, it is not easy to define physically the threshold between the linear viscoelasticity and nonlinear viscoelasticity, so obtaining the exact threshold value still needs further effort. Herein, the assumption is adopted for the comparison with the literature. With all material constants and parameters at each load level being identified by the creep-recovery experiments, the polynomial functions are employed to extrapolate the evolution of the parameters for an arbitrary stress profile. In the present work, D_0 equals 0.107, the calibrated elastic compliance and Prony parameters are given in Table 1. The polynomial functions and corresponding coefficients are presented in Table 2.

Table 1. Parameters of Prony series

n	λ_n	D_n
1	1	1.662×10^{-3}
2	10^{-1}	2.524×10^{-3}
3	10^{-2}	2.527×10^{-3}
4	10^{-3}	4.551×10^{-3}
5	10^{-4}	7.615×10^{-3}
6	10^{-5}	13.366×10^{-3}

Table 2. Parameters of the model

Polynomial function	
$\begin{cases} g_0 = 1 \\ g_0 = 0.972 + 0.442\sigma - 2.029\sigma^2 + 4.687\sigma^3 - 3.616\sigma^4 \end{cases}$	$\begin{matrix} \sigma < 10\%MBL \\ \sigma \geq 10\%MBL \end{matrix}$
$\begin{cases} g_1 = 1.005 - 2.867\sigma + 26.622\sigma^2 \\ g_1 = 5.155 - 9.745\sigma + 3.314\sigma^2 \end{cases}$	$\begin{matrix} \sigma < 30\%MBL \\ \sigma \geq 30\%MBL \end{matrix}$
$\begin{cases} g_2 = 1 \\ g_2 = -0.5 + 15\sigma \\ g_2 = 23.4 - 220.5\sigma + 805.6\sigma^2 - 1281.4\sigma^3 + 745.7\sigma^4 \end{cases}$	$\begin{matrix} \sigma < 10\%MBL \\ 10\%MBL \leq \sigma < 20\%MBL \\ \sigma \geq 20\%MBL \end{matrix}$
$\begin{cases} a_\sigma = 1 \\ a_\sigma = 0.55 + 5.483\sigma - 21.833\sigma^2 + 31.667\sigma^3 - 16.667\sigma^4 \end{cases}$	$\begin{matrix} \sigma < 20\%MBL \\ \sigma \geq 20\%MBL \end{matrix}$
$\begin{cases} D_p = 0 \\ D_p = -0.084 + 1.139\sigma - 4.204\sigma^2 + 6.156\sigma^3 - 3.189\sigma^4 \end{cases}$	$\begin{matrix} \sigma < 20\%MBL \\ \sigma \geq 20\%MBL \end{matrix}$
$\begin{cases} m = 0 \\ m = 0.055 + 2.758\sigma - 18.75\sigma^2 + 39.167\sigma^3 - 25\sigma^4 \end{cases}$	$\begin{matrix} \sigma < 20\%MBL \\ \sigma \geq 20\%MBL \end{matrix}$

VALIDATION OF THE MODEL AND PARAMETRIC ANALYSIS

Comparison between Experimental and Predicted Results

In order to verify the model under creep-recovery loading, the same 33t MBL polyester rope mentioned before but with different loading levels and a longer loading time was employed. In this case, the total loading lasted 136800s; the loading levels are listed in Table 3. The comparison between experimental and predicted results is presented in Fig. 3. It is found that the predicted strain evolution correctly follows the test data but there is a small offset during the process. In order to further understand the offset, an error analysis was carried out and the results are listed in Table 4. It is observed from this table that the relative errors of the predicted results are all within 6.0% whether in the creep or in the recovery processes. The predicted results show a good relativity and confirm the effectivity and veracity of the model.

Table 3. Sequence of loading for parameter identification

t (10^3s)	σ ($\%MBL$)	Time(10^3s)
0-7.2	30	7.2
7.2-61.2	0	54
61.2-66.6	15	5.4
66.6-73.8	40	7.2
73.8-81.0	20	7.2
81.0-88.2	0	7.2
88.2-109.8	50	21.6
109.8-136.8	0	27

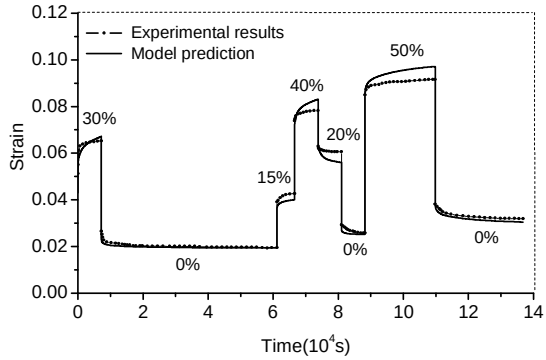

Fig. 3 The comparison between experimental and predicted results

Table 4. Error analysis results

t (s)	σ (%MBL)	$\lvert\varepsilon_e - \varepsilon_m\rvert$ (10^{-3})	Relative error (%)
0-7.2	30	1.233	3.7
7.2-61.2	0	0.640	2.9
61.2-66.6	15	2.489	6.0
66.6-73.8	40	2.420	3.1
73.8-81.0	20	1.861	3.0
81.0-88.2	0	1.431	5.2
88.2-109.8	50	3.989	4.4
109.8-136.8	0	1.238	3.7

The experimental data in the literature (Wibner et al., 2003) were also employed to verify the model under sinusoidal loading. In this case, 900 cycles of the stress-strain hysteresis curve between 25%~55% MBL are presented in Fig. 4, where the middle part of the cycles is ignored. It is evident that in the loading and unloading processes, the hysteresis loop gradually becomes superposed and remains stable after certain cycles. Based on the developed model, we can also obtain 900 cycles of the stress-strain hysteresis loop under the same loadings, i.e., 25%~55% MBL, as indicated in Fig. 5. It can be found that the hysteresis loop is also superposed and becomes stable after certain cycles. This is a property of vital importance of the synthetic fiber ropes under cyclic loading (Bitting, 1985; François and Davies, 2000; Flory et al., 2004; Flory et al., 2007). The last cycle can be clearly seen in Fig. 5 and Fig. 6, which is generally used to calculate the dynamic stiffness of the synthetic fiber ropes. Because it was difficult to find the corresponding stress-strain hysteresis curves of the case mentioned herein, just the qualitative analysis was performed, but it can also illustrate a good relativity and validity of the model.

Through the two loading cases, it is demonstrated that the model can capture the key properties of the synthetic fiber ropes whether under creep-recovery or sinusoidal loadings. However, it should be emphasized that only the qualitative analysis for the sinusoidal loading case was performed due to insufficiency of the test data for the stress-strain hysteresis loops. In fact, there are still uncertainties in describing the hysteresis properties of synthetic fiber ropes. Further complete and integrated model experiments need to be carried out.

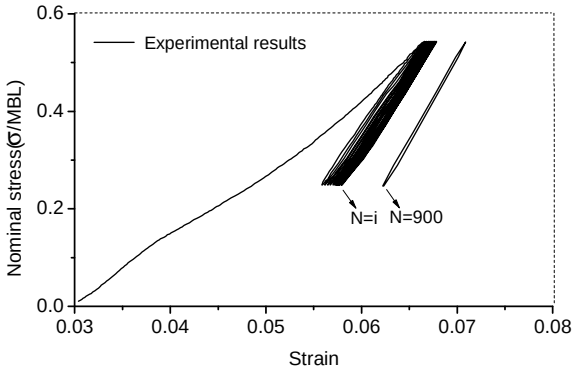

Fig. 4 900 cycles of the stress-strain relationship based on experimental results

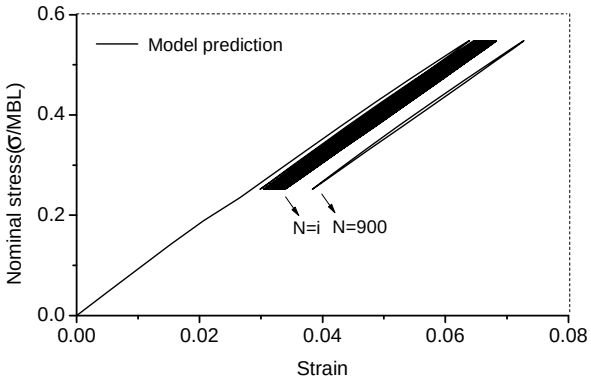

Fig. 5 900 cycles of the stress-strain relationship based on model results

Parametric Analysis

In this section, the parameters of the model including g_0, g_1, g_2, a_σ, D_p and m are investigated in detail through designing six cases. Three values of each parameter are adopted but the others are determined by Table 2. The sinusoidal loading condition is adopted; the mean load L_m equals 20% MBL, the load amplitude L_a equals 10% MBL, and the loading period T equals 10s.

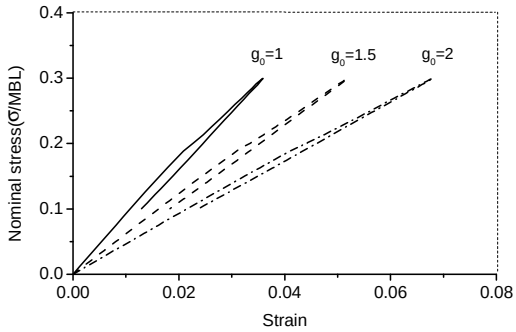

Fig. 6 The influence of g_0 on the stress-strain relationship for a single cycle

The influence of the parameter g_0 on the stress-strain curve for one cycle is presented in Fig. 6. It is indicated that, with the increase of g_0 from 1 to 2, the secant stiffness becomes lower, and the maximum strain under the peak loading and the residual strain of the recovery end in the single cycle become larger. The influence of g_0 on the dynamic

stiffness of 500 cycles loading is presented in Fig. 7. It is observed from this figure that there are no significant increases in the dynamic stiffness and it is almost smooth in the whole loading process. It is due to that the constant is adopted as the value of g_0, thus the nonlinear effect of g_0 is not taken into account. Besides, it can be found that there are significant decreases in the dynamic stiffness with g_0 changing from 1 to 2, because g_0 is the instantaneous elastic compliance, which measures the reduction or increase in the stiffness.

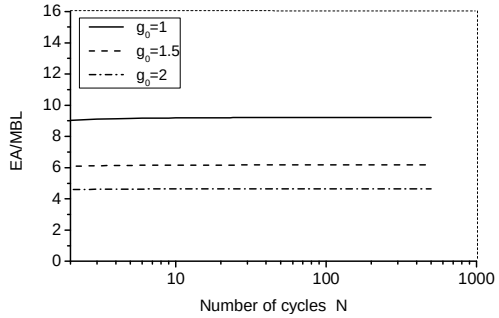

Fig. 7 The influence of g_0 on the dynamic stiffness

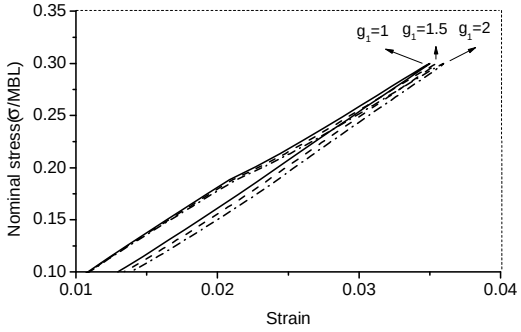

Fig. 8 The influence of g_1 on the stress-strain relationship for a single cycle

The influence of the parameter g_1 on the stress-strain curve for one cycle is shown in Fig. 8. It can be seen that, with the increase of g_1 from 1 to 2, the secant stiffness becomes lower but it can not change more than the case for g_0, and there isn't significant offset on the residual strain for each case at the recovery end. The influence of g_1 on the dynamic stiffness of 500 cycles is shown in Fig. 9. It can be seen that there are nonlinear increases in the dynamic stiffness during the loading cycles and it then becomes stable after certain cycles. With the increase of g_1 from 1 to 2, the dynamic stiffness decreases. It is due to that the transient creep parameter g_1 measures the nonlinear effect in the transient compliance.

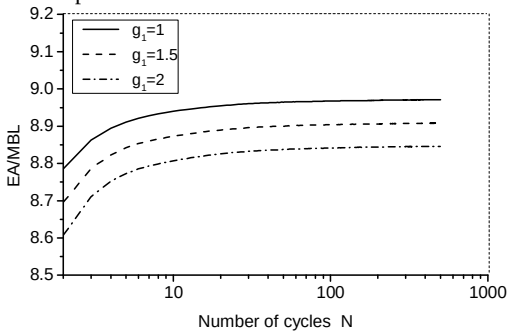

Fig. 9 The influence of g_1 on the dynamic stiffness

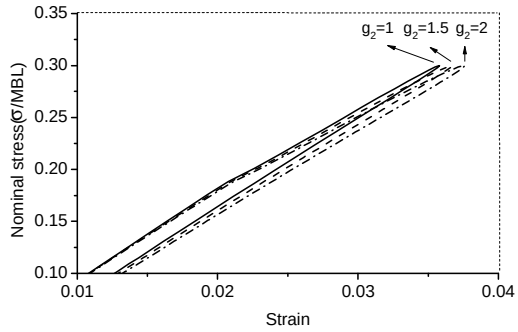

Fig. 10 The influence of g_2 on the stress-strain relationship for a single cycle

The influence of the parameter g_2 on the stress-strain properties for one cycle is shown in Fig. 10. It is evident that the secant stiffness of one cycle becomes lower, and the strain at the peak loading increases larger than the residual stain, with the increase of g_2 from 1 to 2. The strain during the loading and unloading processes increases with an increase of g_2. The influence of g_2 on the dynamic stiffness is presented in Fig. 11. It has the similar effect on the dynamic stiffness as g_1, which is that there are significant decreases in the value of dynamic stiffness with g_2 changing from 1 to 2. It is due to that the increases of the parameters g_1 and g_2 directly make the strain increase.

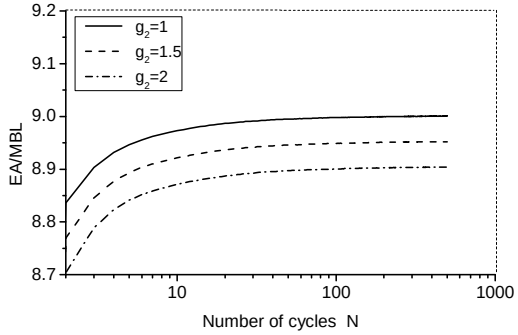

Fig. 11 The influence of g_2 on the dynamic stiffness

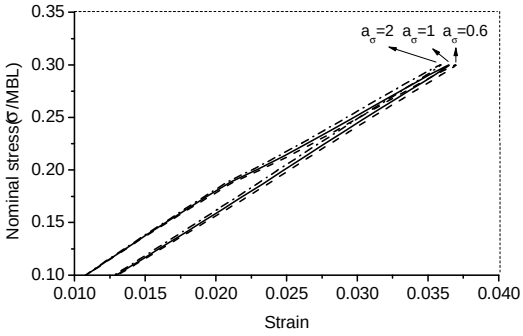

Fig. 12 The influence of a_σ on the stress-strain relationship for a single cycle

The parameter a_σ acts as a time scaling factor. It is observed that the secant stiffness of one cycle becomes larger with the increase of a_σ, as shown in Fig. 12. With the increase of a_σ, the strain at the peak loading decreases more significantly compared with the decrease of the residual strain. The influence of a_σ on the dynamic stiffness of 500 cycles can be seen in Fig. 13. For the parameter a_σ, a similar behavior is apparent, with the increase of a_σ from 0.6 to 2, the dynamic stiffness increases. It is obvious that, with a_σ changing from 0.6 to 2, the reduced time ψ

reduces significantly which decreases the viscoelastic strain, thus the dynamic stiffness increases.

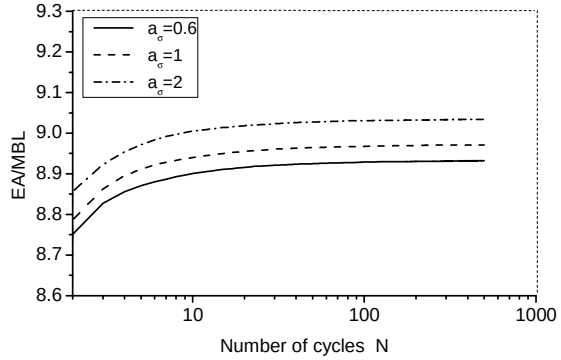

Fig. 13 The influence of a_σ on the dynamic stiffness

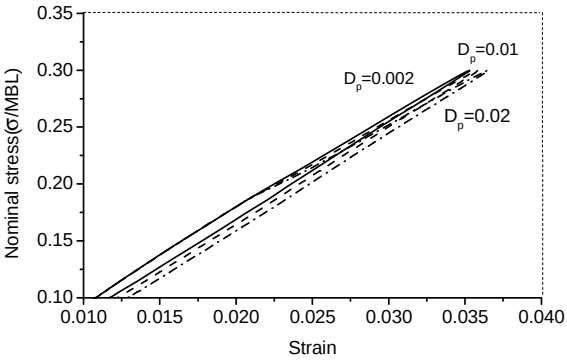

Fig. 14 The influence of D_p on the stress-strain relationship for a single cycle

The plasticity rate D_p and the exponent m are two parameters of the plastic strain in the developed model. The influence of the parameter D_p on the stress-strain properties for one cycle is shown in Fig. 14. It is found that the residual strain significantly increases with the increase of D_p; the strain is only influenced by this parameter when the applied stress is larger than the yield stress; when the stress is lower than the yield stress, the effect from D_p is ignored.

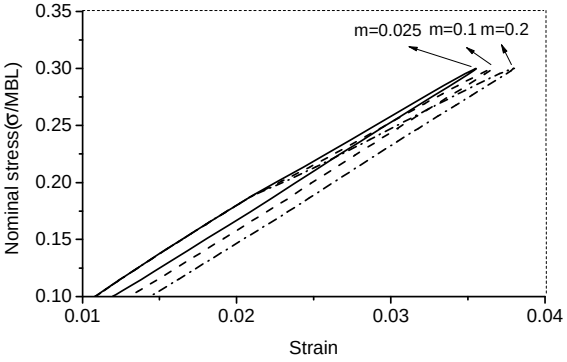

Fig. 15 The influence of m on the stress-strain relationship for a single cycle

The influence of the parameter m on the stress-strain properties for one cycle is shown in Fig. 15. Because m is also the parameter that directly influences the plastic strain, it has the similar effect from the plasticity rate D_p, i.e., only when the stress is larger than the yield stress, the influence of m is taken into account. It is observed that the strain increases with the increase of m from 0.025 to 0.2 and the hysteresis loop becomes larger. This means that the dissipation energy is becoming larger with the increase of m.

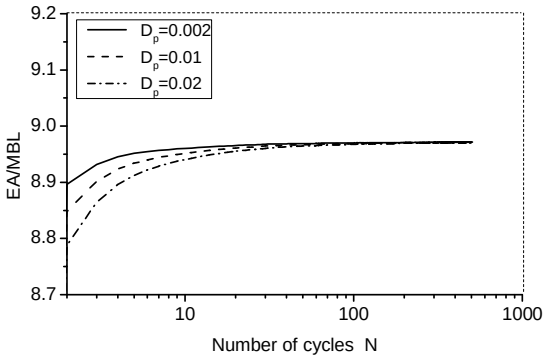

Fig. 16 The influence of D_p on the dynamic stiffness

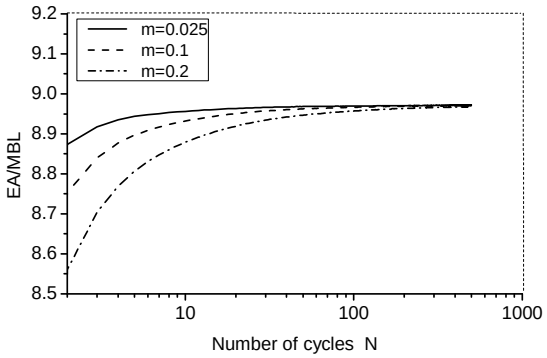

Fig. 17 The influence of m on the dynamic stiffness

The influences of the parameters D_p and m on the dynamic stiffness are presented in Figs. 16 and 17. It is observed from the figures that there are increases in the dynamic stiffness with decreasing values of D_p and m, because the two parameters make the viscoplastic strain significantly increase. Besides, it should be noted that the dynamic stiffness will almost reach a constant in the cases for each parameter. This is due to that the viscoelastic strain covers the main part of the total strain, while a smaller part of the viscoplastic strain is taken into account in the developed model. In the further studies, a more rational viscoplastic theory and computational model are needed to evaluate the plastic strain.

CONCLUDING REMARKS

In this paper, a viscoelastic and viscoplastic model is developed to describe the nonlinear stress-strain properties of the synthetic fiber mooring lines under cyclic loading. How to calculate the tension response of the mooring line precisely under the complicated ocean environment is a key problem to ensure the safety of mooring systems and floating platforms. A stress-strain relationship that directly influences the mooring analysis is urgently needed. It is demonstrated from the former works that the present model and analysis method can not take into account the true loading history, the creep behavior and the dynamic stiffness evolution, which is of vital importance and interest to mooring system designers, platform operators, and researchers. These properties are fully taken into account in the developed model, which are based on the Schapery thermodynamic theory combined with a plastic function.

A new method for the parameter identification, which is essential for a

numerical model, is presented. All the stress-dependent parameters can be determined based on a simple series of creep-recovery experiments of ropes or subropes. It should be noted that the method is capable of analytically evaluating the transient compliance g_1 so that any inaccuracies and instabilities introduced by multiple numerical treatments are avoided.

In order to verify the model, the comparisons between experimental and predicted results both under creep-recovery and sinusoidal loadings are presented. It is found that the relative errors of the predicted results are all within 6.0% whether in the creep or in the recovery processes, which shows a good relativity and confirms the effectivity and veracity of the model. Besides, it is proved that the model can capture the key properties of the synthetic fiber ropes under cyclic loading.

Finally, the influence of parameters on the stress-strain curve for one cycle and the dynamic stiffness evolution is presented. Under sinusoidal loading, the strain in the loading and unloading processes increases with an increase of g_0, g_1 and g_2. This increase meanwhile leads to decreasing of the dynamic stiffness. It is indicated that the decrease of a_σ will make the dynamic stiffness increase. The two parameters of the plastic strain, i.e., D_p and m will make the viscoplastic strain increase significantly, thus there are significant decreases in the dynamic stiffness.

It should be pointed out that the hysteresis is the most important property of the synthetic fiber ropes under cyclic loading due to the complicated viscoelasticity and viscoplasticity. The hysteresis loop consists of two parts, one is the accumulated viscoelastic residual strain, the other is the plastic strain. In fact, there are still uncertainties associated with the hysteresis property and dynamic stiffness evolution under more complicated loading conditions. The present work is beneficial to improving the understanding of the performance of synthetic fiber ropes, and also provides a better basis for the further research on the mechanical problems of synthetic fiber mooring lines. However, further experimental studies are needed to figure out clearly these properties which will be incorporated in the subsequent numerical model.

ACKNOWLEDGEMENTS

Financial support from the National Natural Science Foundation of China (Grant nos. 50979070 and 51179124) is greatly acknowledged. The support of Prof. Dongyan Zhao of COOEC is greatly acknowledged.

REFERENCES

Bitting, KR (1985). "Dynamic modeling of nylon and polyester double braid line", *Oceans conference record*, Vol 17, pp 1344-1353.

Bosman, RLM, Hooker, J, (1999). "The elastic modulus characteristics of polyester mooring ropes", *Proc 31th Annual Offshore Tech Conf*, OTC 10779, Houston, USA.

Casey, NF, Banfield, SJ, (2002). "Full-scale fiber deepwater mooring ropes: advancing the knowledge of spliced systems", *Proc 34th Annual Offshore Tech Conf*, OTC 14243, Houston, USA.

Casey, NF, Belshaw, R, Paton, AG, et al., (2000). "Short- and long-term property behaviour of polyester rope", *Proc 32th Annual Offshore Tech Conf*, OTC 12177, Houston, USA.

Casey, NF, Banfield, SJ, (2005). "Factors affecting the measurement of axial stiffness of polyester deepwater mooring rope under sinusoidal loading", *Proc of the 35th Annual Offshore Technology Conference*, OTC 17068, Houston, USA.

Chailleux, E, Davies, P, (2003). "Modelling the non-linear viscoelastic and viscoplastic behaviour of aramid fibres yarns ", *Mech Time-depend Mat*, Vol 7, pp 291-303.

Chailleux, E, Davies, P, (2005). "A non-linear viscoelastic viscoplastic model for the behaviour of polyester fibres", *Mech Time-depend Mat*, Vol 9, pp 147-160.

Davies, P, Chailleux, E, Bunsell, A, et al., (2003). "Prediction of the long term behavior of synthetic mooring lines", *Proc 35th Annual Offshore Tech Conf*, OTC 15379, Houston, USA.

Davies, P, Francois, M, Grosjean, F, et al., (2002). "Synthetic mooring lines for depths to 3000 meters", *Proc 34th Annual Offshore Tech Conf*, OTC 14246, Houston, USA.

Davies, P, Lechat, C, Bunsell, A, et al., (2008). "Deepwater moorings with high stiffness polyester and PEN fiber ropes", *Proc 40th Annual Offshore Tech Conf*, OTC 19315, Houston, USA.

Del Vecchio, CJM, (1992). Light weight materials for deep water moorings, Ph. D. Dissertation, Reading Univ., UK.

Flory, JF, Ahjem, V, Banfield, SP, (2007). "A new method of testing for change-in-length properties of large fiber-rope deepwater mooring lines", *Proc 39 Annual Offshore Tech Conf. Paper*, OTC 18770, Houston, USA.

Flory JF, Banfield SP, Petruska DJ, (2004). "Defining, measuring, and calculating the properties of fiber rope deepwater mooring lines", *Proc 36 Annual Offshore Tech Conf*, OTC 16151, Houston, USA.

François, M, Davies, P, (2000). "Fibre rope deep water mooring: a practical model for the analysis of polyester systems", *Rio Oil & Gas Conference*, Rio de Janeiro, Brazil.

François, M, Davies, P, (2008). Characterization of polyester mooring lines, *Proc OMAE conference*, OMAE2008-57136, Estoril, Portugal.

François, M, Davies, P, Grosjean, F, et al., (2010). "Modelling fiber rope load-elongation properties - polyester and other fibers", *Proc 42th Annual Offshore Tech Conf*, OTC 20846, Houston, USA.

Haj-Ali, RM, Muliana, AH, (2004). "Numerical finite element formulation of the Schapery non-linear viscoelastic material model", *Int J Numer Meth Eng*, Vol 59, pp 25-45.

Lai, J, Bakker, A, (1995). "An integral constitutive equation for nonlinear plasto-viscoelastic behavior of high-density polyethylene", *Polymer Engineering and Scienc*, Vol 35, No 17, pp 1339-1347.

Lai, J, Bakker, A, (1996). "3-D Schapery representation for non-linear viscoelasticity and finite element implementation", *Comput Mech*, Vol 18, No 3, pp 182-191.

Nielsen, FG, Bindingbø, AU, (2000). "Extreme loads in taut mooring lines and mooring line induced damping: an asymptotic approach", *Applied Ocean Research*, Vol 22, No 2, pp 103-118.

Kim, JS, Muliana, AH, (2009). "A time-integration method for the viscoelastic-viscoplastic analyses of polymers and finite element implementation", *Int J Numer Meth Eng*, Vol 79, pp 550-75.

Schapery, RA, (1969). "On the characterization of nonlinear viscoelastic materials", *Polymer Engineering and Scienc*, Vol 9, No 4, pp 295-310.

Wibner, C, Versavel, T, Masetti, I, (2003). "Specifying and testing polyester mooring rope for the Barracuda and Caratinga FPSO deepwater mooring systems", *Proc Annual Offshore Tech Conf*, OTC 15139, Houston, USA.

Xia, ZH, Shen, XH, Ellyin, F, (2005). "Cycilc deformation behavior of an epoxy polymer, part II: predictions of viscoelastic constitutive models". *Polymer Engineering and Scienc*, Vol 45, No 1, pp 103-113.

Ye, Y, Yang, XH, Chen, CY, (2010). "Modified Schapery's model for asphalt sand", *J Eng Mech*, Vol 136, No 4, pp 448-454.

Zapas, LJ, Crissman, JM, (1984). "Creep and recovery behaviour of ultra-high molecular weight polyethylene in the regin of small uniaxial deformations", *Polymer*, Vol 25, No 1, pp 57-62.